



Role of pyrolysis temperature on application dose of rice straw biochar as soil amendment

Subham C. Mondal¹ · Banashree Sarma¹ · Rumi Narzari² · Lina Gogoi² · Rupam Kataki² · Ankit Garg³ · Nirmali Gogoi¹

Received: 12 October 2020 / Revised: 26 January 2022 / Accepted: 5 February 2022 / Published online: 13 March 2022
© The Author(s) under exclusive licence to Society for Environmental Sustainability 2022

Abstract

Biochar, an emerging soil amendment is conducive to carbon sequestration as well as plant and soil health. However, its benefits vary with the type of feedstocks, pyrolysis temperature, and the rate of application in soil. Herein, the effects of pyrolysis temperature and application dose of rice straw-derived biochar on soil physico-chemical properties were investigated. In this study, biochar prepared at two pyrolysis temperatures (350 °C and 550 °C) were applied in the soil at the rate of 5%, 10%, and 20%. After 90 days of incubation (at 50% of water holding capacity), a significant increase in soil pH and loss of nitrogen (up to 80%) was observed in biochar applied soils along with enhanced availability of phosphorous (14%) and potassium (18.8 fold). The addition of biochars (derived at both the temperatures) at a dose of 20%, elevated the carbon mineralization rate. Results demonstrated the crucial role of both pyrolysis temperature and application rate in achieving optimum efficacy of rice straw-derived biochar in soil carbon mineralization. The study suggests that rice straw biochar prepared under low (350 °C) pyrolysis temperature should be applied at a lesser rate (5%) to obtain higher agronomic and environmental benefits. Whereas, a higher rate of application (10%) is advocated if the pyrolysis is performed at a higher temperature (550 °C).

Keywords Rice straw-derived biochar · Mineralization · Pyrolysis temperature · Application dose

Introduction

Biochar is recommended as a soil amendment in agriculture to improve crop production (Reed et al. 2016). Earlier studies established that organic structures such as water-soluble organics, aliphatics with high molecular weight, and relatively high content of insoluble aromatic structures in biochar pose an impact on soil properties (Brennan et al. 2014; Buss et al. 2015). The presence of these compounds in the soil helps in microbial growth by acting as a suitable substrate (Ameloot et al. 2013). This enhances the microbial biomass as well as diversity in the soil (Kolb et al. 2009). The degradation of polycyclic aromatic hydrocarbons in the soil (Zhang et al. 2018) results in better crop performances. Moreover, precipitation of these molecules contributes to long-term soil carbon (C) storage by forming larger molecules as only 10–20% of the soluble content is mineralized to CO₂ (Smith et al. 2010). Thus, the application of biochar largely affects the structure, stability, nutrient dynamics, aeration and C storage capacity in soil (Lehmann et al. 2011). The inert nature of biochar towards

✉ Nirmali Gogoi
nirmalievs@gmail.com

Subham C. Mondal
xubham@gmail.com

Banashree Sarma
banashree07@gmail.com

Rumi Narzari
pinkilkt@gmail.com

Lina Gogoi
lina.dbr@gmail.com

Rupam Kataki
rupam@tezu.ernet.in

Ankit Garg
ankit@stu.edu.cn

¹ Department of Environmental Science, Tezpur University, Tezpur, Assam 784 028, India

² Department of Energy, Tezpur University, Tezpur, Assam 784 028, India

³ Department of Civil and Environmental Engineering, Shantou University, Shantou, China

chemical and biological degradation is highly investigated for its carbon sequestration potential (Singh et al. 2010; Sagrilo et al. 2015; El-Naggar et al. 2018). The physico-chemical properties of biochar determine carbon mineralization potential and it changes with the feedstock material and pyrolysis condition (Antal and Grønli 2003; Gaskin et al. 2008). Increased cumulative CO₂ efflux was reported due to enhanced microbial activity under the application of mixed crop residue biochar prepared at 500 °C (El-Naggar et al. 2018). However, earlier studies documented contrasting results in microbial activity from the addition of biochar due to the differences in soil type, application rate, and intrinsic properties of feedstock (Kuzuyakov et al. 2009; Warnock et al. 2010). Mukherjee et al. (2014) and Singh et al. (2012) also confirmed the role of pyrolysis temperature upon soil C mineralization. Furthermore, it has been documented that increasing application dose of peanut shell biochar increases the C mineralization rate in soil (Luo et al. 2011). As biochar is not completely biologically inert, CO₂ emission from the soil as a result of degradation of labile aliphatic C become prominent (Liang et al. 2008). In the long term, this influences the C sequestration potential of the applied biochar. Maestrini et al. (2014) reported that biochar rich in labile C matter induces a short-term positive effect upon the native soil organic C but in the long term, a negative effect is observed because of increased C mineralization rate. This increased C mineralization rate and degradation of labile C may be beneficial for agricultural crop health (Ventura et al. 2014) but CO₂ emission has negative consequences for the environment. This demands the importance of determining the availability and extraction of labile C present in the biochar to maintain optimal C mineralization to reap benefits as preferred.

Therefore, determining the ideal pyrolysis temperature and application dose of biochar for a specific feedstock is crucial for achieving the maximum benefit as a soil amendment. A plethora of work has been reported regarding the effects of the pyrolysis environment on biochar quality for obtaining optimum application rate of biochar for C mineralization (Liu et al. 2018). However, studies concerned with the interaction effect of both conditions are scanty. According to Lefevre et al. (2014), laboratory incubation with standardized conditions is an effective method to examine C mineralization. With this perspective, a laboratory incubation study was conducted with rice straw as a feedstock of biochar using two pyrolysis temperatures (350 °C and 550 °C), which was applied to the soil at three levels. We hypothesized that the production temperature of biochar is important for its application as a soil amendment. Our objective was to screen the pyrolysis temperature and application dose of biochar on the basis of soil physico-chemical properties and C mineralization.

Materials and methods

Feedstock material

Rice straw was collected from the farmers' field in the vicinity of Tezpur University campus, Napaam, Assam, India (Coordinates: 26°41'N and 92°50'E). After the collection (during January 2017), biomass was washed thoroughly and sun-dried, chopped, and grounded in a willy mill (SECOR Scientific Eng. Co). Powdered samples were sieved through a 0.2 mm sieve and then oven-dried.

Biochar preparation

Biochar was prepared in a fixed bed lab-scale pyrolyzer (Montech Instruments, Chandigarh, India). Biomass sample (10 g) was fed into the tubular quartz reactor and heated at two pyrolysis temperatures, i.e., 350 °C and 550 °C with a heating rate of 40 °C/min under nitrogen flow of 100 ml/min. The residence time for pyrolysis was kept as 3 min.

Soil preparation/sampling

The soil was collected from an agricultural field near the Tezpur university campus (26°41'N and 92°50'E), air-dried, homogenized, and sieved to pass a 2-mm sieve. The soil was sandy loam in texture. The recorded pH, bulk density, water-holding capacity, and cation exchange capacity of the experimental soil were 5.69, 1290 kg m⁻³, 44.4%, and 12.24 (cmol⁺ kg⁻¹) respectively.

Incubation study

The study was performed in the laboratory using 500 mL polyethylene bottles, taking 50 g of soil as control. Biochar was mixed with soil at three levels, i.e., 5%, 10%, and 20% w/w; the control group was soil-only (UC); all the treatments were replicated thrice (Fig. 1). The samples were placed in a Biological Oxygen Demand (BOD) incubator (BD Instrumentation India-Labotech BD-55) accommodating three replications of each treatment along with control in a completely randomized design (CRD). Incubation was done at 25 °C temperature for 90 days. Initially, the rate of CO₂ emission was determined daily for the first 5 days, intervals of every 5 days for the next 25 days, and every 10 days for the last 60 days. Produced CO₂ was trapped in 0.05 M NaOH (10 mL) and titrated against 0.05 M HCl after adding 10 ml of BaCl₂ and a few drops of phenolphthalein indicator. The end-point was achieved when the titrate color changed from pink to white. Cumulative CO₂

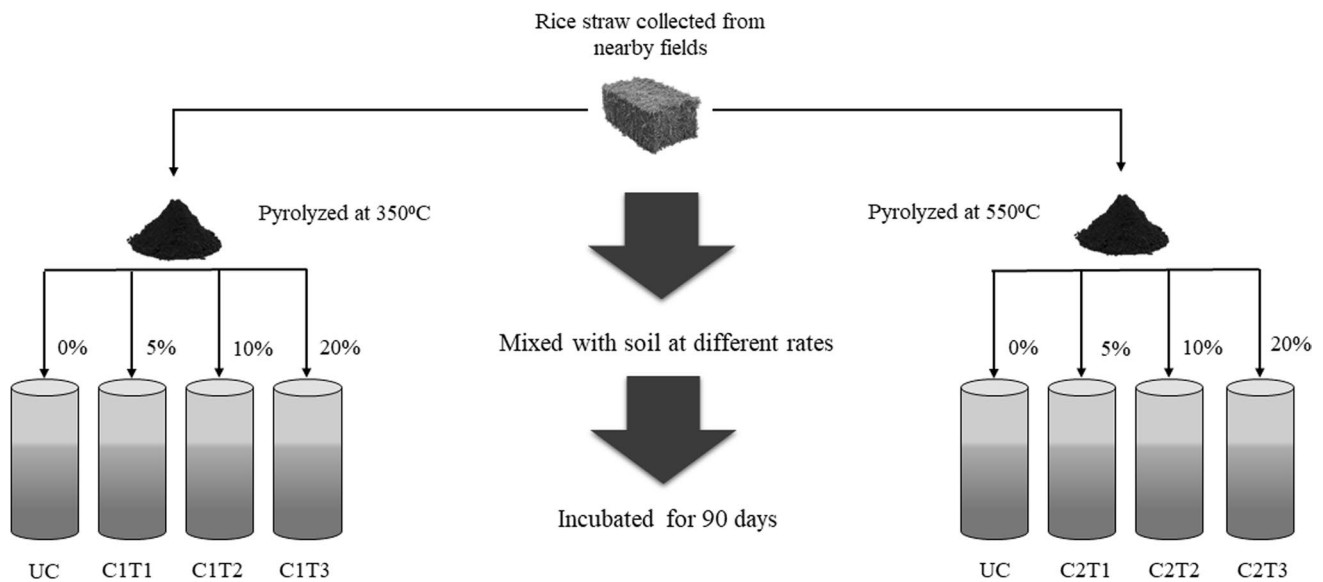


Fig. 1 Experimental design of the study conducted. UC=Control; C1=Biochar produced at 350 °C; C2=Biochar produced at 550 °C; T1=5% biochar application; T2=10% biochar application; T3=20% biochar application

emission was calculated by adding the emissions until the end of the experiment (90 days).

Determination of physico-chemical properties of biochar

The quantitative elemental analysis for carbon (C), hydrogen (H), and nitrogen (N) of biochar samples were carried out using an elemental analyzer (PE 2400 C, H, N analyzer, Perkin Elmer). Moisture (M), ash, volatile matter (VM), and fixed carbon (FC) content were determined using ASTM methods, viz. ASTM D3173-87 (ASTM D3173/D3173M-17a 2017), ASTM D3174-12 (D3174-12 2018), ASTM D3175-18 (ASTM D3175-18 2018) and ASTM D1106-21 (ASTM D1106-21 2017) respectively. The percentage of oxygen was identified by using the following equation (Eq. 1), as per Huff et al. (2018).

$$\text{Oxygen} = 100 - (\text{Carbon}\% + \text{Hydrogen}\% + \text{Nitrogen}\%) \quad (1)$$

Molar elemental ratios such as H/C and O/C are useful in organic elemental analysis. These ratios were calculated by using atomic weight and percent weight of the respective elements. CHN Elemental Analyzer was used to obtain the element percent and the atomic weight of the elements (Culmo et al. 2013; Kong et al. 2019). The element ratios, H/C and O/C were calculated as follows:

$$\text{H/C} = \frac{\frac{\text{Weight Percent Hydrogen}}{\text{Atomic Weight Hydrogen}}}{\frac{\text{Weight percent carbon}}{\text{Atomic weight carbon}}}, \text{O/C} = \frac{\frac{\text{Weight Percent Oxygen}}{\text{Atomic Weight Oxygen}}}{\frac{\text{Weight percent carbon}}{\text{Atomic weight carbon}}}$$

The IR spectra of the samples were recorded on a Nicolet IR spectrometer at room temperature (26 ± 2 °C). A region in the spectral range of $4000\text{--}400\text{ cm}^{-1}$ was used for analysis. Qualitative analysis for the elements present in the biochar samples was performed by means of scanning electron microscopy with energy dispersive X-ray spectroscopy (SEM-EDX) (JEOL Japan- JSM 6390LV) spectra.

Determination of soil chemical properties

The pH of the samples was recorded using a pH meter (HI96107, Hanna Instruments, Australia). Bulk density was determined by weighing the soil in a known volume of bulk density bottles (ASTM D1895-17 2017). Soil available nitrogen (N), potassium (K), and phosphorus (P) were estimated at the end of the incubation period through the micro Kjeldahl method proposed by Subbiah and Asija, (1956), the flame photometric method by Jackson (1958), and the spectrophotometric method by Bray and Kurtz (1945) respectively. Soil humic acid (HAC) and fulvic acid carbon (FAC) were estimated as suggested by Page

et al. (1982). Soil microbial biomass carbon (MBC) was determined using the CHCl_3 fumigation extraction method as given by Vance et al. (1987).

Statistical analyses

The data sets were processed for analysis of variance (ANOVA). Significant differences among treatment means of three replicates ($n=3$) and the least significant difference (LSD) at a 5% level of probability were calculated using SPSS for Windows 16.0. The graphical representation of the data was made using Graphpad Prism 7.

Results

Proximate and ultimate analyses

Addition of 5% biochar obtained at 350 °C pyrolysis temperature reduced H (34%), N (46%), O (15%), the ratio of O/C and H/C, M%, VM (21%), and FC (21%) content (Table 1) whereas, C% was enhanced (15%). Increasing application dose (10%) of the same biochar recorded enhanced O% (30%), O/C ratio, with reduced C% (Table 1). Further increase of application dose to 20% resulted in a greater reduction in H/C ratio and M%. Biochar obtained at higher pyrolysis temperature (550 °C) reduced C% (1.4%) even under lower application dose (5%). However, improvement in H% (66%), O% (0.85%), H/C, and O/C was noted under this condition. Application of same biochar at higher doses (10% and 20%) documented even greater content of H% (up to 25%), H/C, ash% (up to 16%), and M% with lesser VM (up to 27%) content. Reduction in O% (13%), O/C, and FC

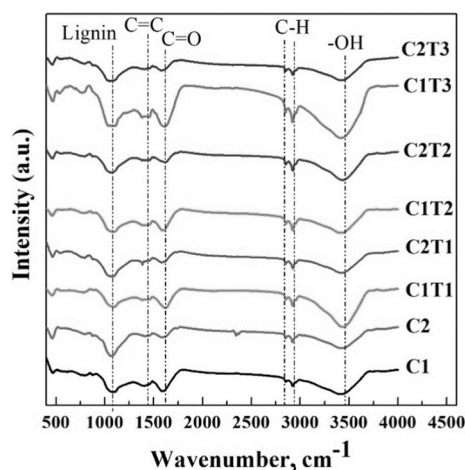


Fig. 2 FTIR spectra of rice straw biochars as affected after 90 days of incubation. C1 = Biochar produced at 350 °C; C2 = Biochar produced at 550 °C; T1 = 5% biochar application; T2 = 10% biochar application; T3 = 20% biochar application

(5%) was recorded under the highest application dose of 20%.

Infrared spectral functional group identification and quantification

Irrespective of the pyrolysis temperatures and application doses, FTIR spectra of biochar samples (both pre- and post-incubation) showed broad and strong adsorption peak around 3600–3300 cm^{-1} , indicating the presence of O–H group (Fig. 2). Two weak bands documented at 2920 and 2848 cm^{-1} were assigned to alkyl C–H. A weak band at 2334 cm^{-1} was found only in initial high temperature pyrolyzed biochar (C2) indicating the presence of $\text{C}\equiv\text{N}$.

Table 1 Proximate and ultimate analysis of rice straw biochars after 90 days of incubation

| Treatments | C% | H% | N% | O% | H/C | O/C | M% | Ash% | VM% | FC% |
|------------|---------------------------|--------------------------|--------------------------|---------------------------|------|------|-------|---------------------------|--------------------------|---------------------------|
| C1 | 54.15 ^f ± 0.09 | 3.85 ^b ± 0.03 | 2.92 ^b ± 0.01 | 39.08 ^c ± 0.05 | 0.85 | 0.54 | 10.31 | 22.55 ^h ± 0.03 | 19.5 ^a ± 0.03 | 47.64 ^c ± 0.02 |
| C2 | 58.33 ^d ± 0.06 | 2.62 ^f ± 0.00 | 3.83 ^a ± 0.02 | 35.22 ^f ± 0.01 | 0.54 | 0.45 | 6.92 | 28.09 ^g ± 0.02 | 15.8 ^d ± 0.03 | 49.19 ^b ± 0.01 |
| C1 | | | | | | | | | | |
| T1 | 62.75 ^b ± 0.09 | 2.53 ^g ± 0.02 | 1.57 ^e ± 0.02 | 33.15 ^g ± 0.09 | 0.48 | 0.40 | 6.79 | 34.26 ^d ± 0.06 | 15.3 ^e ± 0.17 | 43.64 ^e ± 0.06 |
| T2 | 46.25 ^g ± 0.06 | 2.29 ^h ± 0.03 | 0.65 ^g ± 0.00 | 50.81 ^b ± 0.06 | 0.59 | 0.82 | 6.72 | 39.62 ^a ± 0.02 | 18.8 ^b ± 0.03 | 34.86 ^h ± 0.01 |
| T3 | 26.58 ^h ± 0.12 | 3.46 ^c ± 0.03 | 1.57 ^e ± 0.02 | 68.39 ^a ± 0.06 | 1.56 | 1.93 | 7.17 | 36.05 ^b ± 0.02 | 16.6 ^c ± 0.17 | 40.18 ^g ± 0.02 |
| C2 | | | | | | | | | | |
| T1 | 57.47 ^e ± 0.03 | 4.35 ^a ± 0.03 | 2.66 ^d ± 0.02 | 35.52 ^e ± 0.02 | 0.91 | 0.46 | 6.78 | 35.31 ^c ± 0.06 | 15.8 ^d ± 0.07 | 42.11 ^f ± 0.06 |
| T2 | 58.67 ^c ± 0.12 | 3.30 ^d ± 0.02 | 1.75 ^d ± 0.02 | 36.28 ^d ± 0.02 | 0.67 | 0.46 | 7.05 | 29.41 ^f ± 0.02 | 11.4 ^g ± 0.23 | 52.14 ^a ± 0.06 |
| T3 | 65.55 ^a ± 0.12 | 3.01 ^e ± 0.02 | 0.96 ^f ± 0.01 | 30.48 ^h ± 0.03 | 0.55 | 0.35 | 7.97 | 32.71 ^e ± 0.06 | 12.9 ^f ± 0.03 | 46.42 ^d ± 0.03 |

C1 = Biochar produced at 350 °C; C2 = Biochar produced at 550 °C; T1 = 5% biochar application; T2 = 10% biochar application; T3 = 20% biochar application; VM = volatile matter; FC = Fixed carbon

*Different lower case letters superscripted to mean values indicate significant differences between treatments at 5% level of significance according to DMRT; Data reported as (mean ± SE), $n=3$

Irrespective of the treatments, the presence of C=O stretch of polysaccharides and Si–O stretch was confirmed by the observed broad and weak band at 1619 cm^{-1} . The weak band obtained at 1439 cm^{-1} represented C=C stretch in the aromatic ring whereas, in all the treatments with the band at 1078 cm^{-1} showed the presence of lignin. Smoothing of bands in the fingerprint region (500–1500 cm^{-1}) indicated the reducing quantity of complex compounds due to thermal degradation. Two strong bands between 2950 and 2800 cm^{-1} (assigned to asymmetric C–H and symmetric C–H bands respectively) proved the presence of aliphatics, olefinics, and aromatics in all the treatments. Likewise, the presence of carbonyls, ketones, aldehydes, or ester groups were verified with the documented stretching absorption band between 1750 and 1600 cm^{-1} attributed to C=O and C=C. Further confirmation on the presence of aromatic structure was obtained by significantly strong absorption bands around

1060 to 1100 cm^{-1} , showing the presence of lignin. Post incubated biochars confirmed the presence of phenols, alcohols, and carboxylic acids with wide and strong –OH stretching bands between 3400 and 3300 cm^{-1} . In addition, the broad band related to hydrogen bonding in the samples verified the presence of water content.

Elemental identification and qualitative compositional properties

The EDX spectra of pre-incubated biochars (C1 and C2) confirmed the presence of C, O, calcium (Ca), magnesium (Mg) and chlorine (Cl) on their surfaces (Table 2). Though K was not detected in the samples, sodium (Na) and iron (Fe) were found in biochars produced at 550 °C and 350 °C respectively. The EDX spectra of the biochar samples after incubation proved the presence of C, O, K, Ca, Mg, Cl, Na,

Table 2 EDX spectrum of the rice straw biochars after 90 days of incubation

| Treatments | Weight percentage | | | | | | | |
|------------|-------------------|-------|------|------|------|------|------|------|
| | C | O | K | Ca | Mg | Cl | Na | Fe |
| C1 | 70.16 | 18.00 | – | 0.26 | 0.19 | 4.76 | – | 6.62 |
| C2 | 72.94 | 21.68 | – | 0.35 | 0.25 | 0.41 | 4.38 | – |
| C1 | | | | | | | | |
| T1 | 65.15 | 31.39 | 0.98 | 1.05 | 0.39 | 0.27 | 0.07 | 0.27 |
| T2 | 74.96 | 20.03 | 2.82 | – | 0.21 | 0.41 | 1.09 | 0.17 |
| T3 | 67.38 | 27.78 | 2.28 | 0.92 | 0.58 | 0.27 | 0.13 | 0.22 |
| C2 | | | | | | | | |
| T1 | 72.74 | 20.33 | 2.94 | 0.83 | 0.52 | 0.26 | 0.19 | – |
| T2 | 74.62 | 23.98 | 0.54 | – | 0.28 | 0.16 | 0.05 | 0.04 |
| T3 | 62.18 | 32.85 | 2.94 | – | 0.59 | 0.57 | 0.30 | 0.06 |

C1 = Biochar produced at 350 °C; C2 = Biochar produced at 550 °C; T1 = 5% biochar application; T2 = 10% biochar application; T3 = 20% biochar application

Table 3 pH, Bulk density and Available N P K of soil as effected under application of biochar during incubation

| Treatments | pH | Bulk Density (g CC^{-1}) | Available N (kg ha^{-1}) | Available Phosphate (mg/kg) | Available K (g kg^{-1}) |
|------------|------|------------------------------------|------------------------------------|-----------------------------|-----------------------------------|
| UC | 7.0 | 1.29 | 250.88 ^a ± 1.31 | 5.91 ^b ± 0.41 | 1.40 ^d ± 0.26 |
| C1 | | | | | |
| T1 | 8.4 | 1.06 | 50.53 ^c ± 1.15 | 5.89 ^b ± 0.03 | 6.30 ^c ± 0.24 |
| T2 | 10.2 | 0.88 | 75.34 ^c ± 1.69 | 6.22 ^{ab} ± 0.27 | 11.10 ^b ± 0.57 |
| T3 | 10.8 | 0.65 | 61.93 ^d ± 1.05 | 6.88 ^a ± 0.19 | 26.40 ^a ± 0.25 |
| C2 | | | | | |
| T1 | 9.5 | 1.17 | 62.56 ^d ± 1.67 | 5.75 ^b ± 0.08 | 5.60 ^c ± 0.26 |
| T2 | 10.1 | 0.86 | 82.52 ^b ± 0.89 | 5.73 ^b ± 0.15 | 11.27 ^b ± 0.29 |
| T3 | 10.8 | 0.66 | 62.52 ^d ± 1.23 | 6.27 ^{ab} ± 0.12 | 26.04 ^a ± 0.25 |
| LSD | | | 1.8 | 0.3 | 0.46 |

UC = Control; C1 = Biochar produced at 350 °C; C2 = Biochar produced at 550 °C; T1 = 5% biochar application; T2 = 10% biochar application; T3 = 20% biochar application

*Different superscript lower case letters within each column indicate significant differences between treatments at 5% level of significance according to Duncan's multiple range test (DMRT). Data reported as (mean ± SE), n = 3

and Fe elements on their surfaces. However, absence of Fe was observed under the addition of lower doses (5%) of high-temperature pyrolyzed biochar (C2T1). Irrespective of the pyrolysis temperature, the absence of Ca was noted in post incubated biochar samples under the application dose of 10%. However, low temperature (350 °C) pyrolyzed biochar documented the highest C content under the same application dose (C1T2).

Soil physico-chemical properties and carbon fractions

Regardless of the pyrolysis temperature, a higher application dose increased soil pH and decreased soil bulk density (Table 3). Biochar addition resulted in significant loss of N with the highest (80% of control) under the treatment C1T1 followed by C1T2 (76% of control). In addition, significant enhancement of soil P and K content was found due to biochar application. The highest available soil P (14%) and K (18-fold) contents were recorded in treatment C1T3 after application of low temperature pyrolyzed biochar at a rate of 20%. Irrespective of the pyrolysis temperature, the highest HAC content (5%) was recorded under the application dose of 20% (Fig. 3). Whereas, biochar obtained at 350 °C pyrolysis temperature documented the lowest HAC content when applied at a rate of 10%. In contrast, higher FAC content (21%) was noted under application of higher doses of (10%

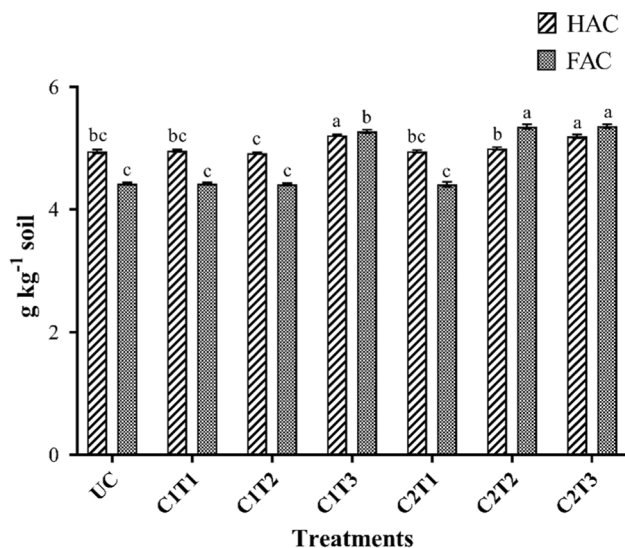


Fig. 3 Effect of rice straw biochar on humic acid carbon and Fulvic acid carbon of the soil. UC=Control; C1= Biochar produced at 350 °C; C2= Biochar produced at 550 °C; T1=5% biochar application; T2=10% biochar application; T3=20% biochar application. *Different lowercase letters above each column indicate significant differences between treatments at 5% level of significance according to DMRT. Error bars on each data points represents standard error in each data point

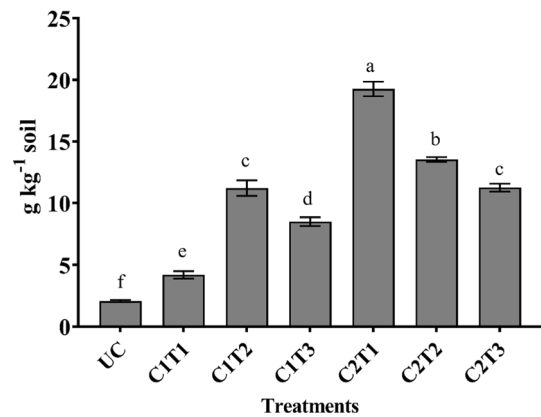


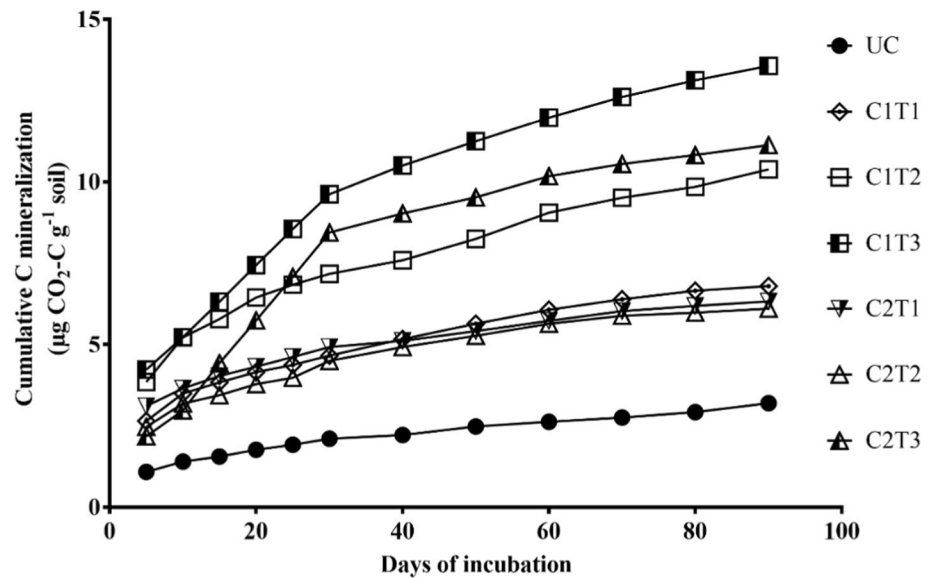
Fig. 4 Effect of rice straw biochar on microbial biomass carbon of the soil. UC=Control; C1= Biochar produced at 350 °C; C2= Biochar produced at 550 °C; T1=5% biochar application; T2=10% biochar application; T3=20% biochar application. *Different lowercase letters above each column indicate significant differences between treatments at 5% level of significance according to DMRT. Error bars on each data points represents standard error in each data point (n = 3)

and 20%) high-temperature pyrolyzed biochars. Pyrolysis temperature had a positive influence on MBC content of the rice straw-derived biochars with 5.4-fold increase under 5% application dose of high temperature pyrolyzed biochar (Fig. 4). Increased biochar application does exert a positive influence on soil C mineralization with the highest under the application of rice straw biochar obtained at low pyrolysis temperature (Fig. 5). Compared to control, all biochar treated soils documented the highest C mineralization rate during the first 30 days of incubation accounting for 67–77% of the total C mineralization that declined afterward.

Discussion

The recorded reducing trend of soil bulk density with the increased application of biochar indicates improved soil aeration (Kumari et al. 2021) and confirms rice straw-derived biochar as an efficient soil conditioner by improving the aerobic microbial diversity. Reduced soil N content under biochar application reveals the stimulating effect of biochar on N loss due to denitrification. Singh et al. (2010) also reported a positive role of biochar in N₂O emission from soils. However, this escalated denitrification is reported to be sporadic and subsides shortly after (Beare et al. 2009). The recorded non-significant differences of P availability across the treatments indicate the positive influence of rice straw-derived biochar in P solubility, which might be attributed to the adsorption of P in biochar surfaces (Takaya et al. 2016). Singh et al. (2010) also reported a positive role of biochar in N₂O emission from soils.

Fig. 5 Effect of rice straw biochar on soil carbon mineralization. UC=Control; C1=Biochar produced at 350 °C; C2=Biochar produced at 550 °C; T1=5% biochar application; T2=10% biochar application; T3=20% biochar application; Error bars on each data points represents standard error in each data point (n = 3)



It is documented that pyrolyzing crop residues help in conversion of organic P to inorganic form such as orthophosphates and pyrophosphates (Chirone et al. 2000) leading to slow release of P by acting as a stable source of P (Dai et al. 2017). The increased availability of soil K content under biochar application reveals the growth of K-solubilizing bacteria that enhance the release of K (Wang et al. 2018). Earlier researchers also reported increased availability of soil K due to biochar addition (Oram et al. 2014; Haque et al. 2021). The alkaline nature of biochar was responsible for increasing soil pH from 1.4 to 3.8 units after 90 days of incubation with the highest value under higher application dose. The presence of different fractions of C (aromatic, aliphatic, volatile matter, labile carbon, etc.) in the biochar provides nutrition to the microorganisms and contributed to the availability of soil nutrients (Alaylar et al. 2021). Moreover, microbial community composition is also sensitive to alteration in soil pH and bulk density (Puissant et al. 2019). However, all these contributing factors of soil physico-chemical properties are determined by the application dose and pyrolysis temperature of the produced biochar.

The availability of labile C, volatile matter, or water-soluble compounds such as aldehydes, ketones, and carboxyl groups in the applied biochars provide the required nutrition for microbial growth and thus help in quicker degradation of C (Ameloot et al. 2013; Egamberdieva et al. 2020). The recorded higher MBC in post-incubated biochar treated soils also confirms this. Promotion of maximum microbial growth under application of 5% and 10% doses of high temperature pyrolyzed biochars might be due to higher surface area and labile C providing favorable conditions for microbes as observed earlier (Ma et al. 2019). The MBC content of the soil is an indication of the soil organic C status (Pei et al. 2017) as labile C in the biochar is used as a source

of C for microbial growth. The absence of alkyl groups in the biochars after incubation indicates its utilization by the microbial communities (Luo et al. 2011). Moreover, higher content of humic and fulvic acid C in biochar-treated soil proves the role of biochar in the improvement of soil stable C content, thus, augmenting extraction of aliphatic C for microbial activity (Horáček et al. 2014). Dai et al. (2017) also confirmed the crucial role of aliphatic C in enhancing soil microbial communities. The studied biochars showed a wide range of functional groups due to the presence of cellulose, hemicellulose, and lignin in the feedstock with an abundance of C, H, and O (Chen et al. 2014). The observed O–H stretching, carbonyls, ketones, and ester groups are consistent with the previous studies of Xiao et al. (2014), Binh and Nguyen (2020) and Bouaik et al. (2021). The presence of the aromatic group indicates dehydrogenation and dehydroxylation of carbohydrates during thermal cracking in absence of oxygen (Keiluweit et al. 2010). Thus, pyrolytic degradation of phenolic acids present in the rice straws is responsible for the documented phenolic stretching in the biochars (Cui et al. 2019). Moreover, the presence of higher silicon (Si) content in the feedstock resulted in the Si–O groups in the tested biochars. The calculated value (0.4–0.5) of the degree of polarity (O/C ratio) of rice straw-derived biochar used in this experiment designates a mean residence time of 100–1000 years as suggested by Spokas (2010). However, the recorded higher degree of polarity from the application of higher doses of low temperature pyrolyzed biochars (20% followed by 10%) indicates lower sequestration potential due to higher C mineralization and low aromaticity as documented from higher H/C ratio (Brassard et al. 2017; Sarfaraz et al. 2020). By contrast, significantly lower degree of polarity reveals higher C sequestration potential of applied biochar when produced at high temperature

(550 °C). The highest degree of polarity (> 1) observed in post-incubated low temperature pyrolyzed biochar especially from the highest application dose (20%) might be due to higher cation exchange capacity, providing a favorable environment for oxidation (Tsai and Chang 2020).

The highest C mineralization observed during the initial 30 days of incubation indicates an active mineralization process due to biochar addition. This initial enhancement in cumulative C mineralization is possibly due to the presence of labile organic compounds, especially in low-temperature pyrolyzed biochars (Sarfaraz et al. 2020). The subsequent reduction in C mineralization rates can be attributed to the air–water balance of the experimental setup and the liming properties of biochar which could have absorbed the released CO₂ together with the slow degradation of aromatic rings (Ameloot et al. 2013; Sarfaraz et al. 2020). Similar results were observed by Luo et al. (2011), where the application of peanut shell biochar accelerated the cumulative carbon mineralization during the initial 40 days and stabilized thereafter.

The application of organic amendments affects soil C dynamics through the process of mineralization and immobilization. Soil carbon mineralization is the CO₂ efflux from soil metabolic processes where the rate of decomposition is affected by various soil properties which vary from place to place (Ventura et al. 2015). Some other researchers observed suppression of soil mineralization under biochar application due to amelioration of soil physico-chemical properties like pH, high surface area, etc. (Yousaf et al. 2017). However, in the present study, higher cumulative C mineralization was observed in all the biochar treatments as compared to control. The effect of the production temperature of biochar on the rate of soil C mineralization was significant with the lowest rate of C mineralization from high temperature produced biochar. This result can provide some baseline information in terms of the production temperature of biochar while optimizing the rate of biochar application that sustainably preserves the soil C pool.

Conclusion

Pyrolysis temperature and application dose of biochar play a crucial role in soil physico-chemical properties and carbon mineralization. Biochar produced at a higher temperature are efficient C sequesters even at a lower dose. Therefore, to obtain the maximum benefit of the applied biochar, optimization of biochar dose with respect to pyrolysis temperature is important. However, long-term field studies in different soil types are needed to understand the role of climatic parameters along with applied nutrients and soil–plant interactions in C mineralization.

Acknowledgements We would like to thank Sophisticated Analytical Instrumentation Center (SAIC), Department of Energy and Department of Environmental Science, Tezpur University, for providing the instrumentation facility required for this study.

Funding No funding was received for this study.

Availability of data and material Data will be made available on request.

Code availability Not applicable.

Declarations

Conflict of interest On behalf of all authors, the corresponding author states that there is no conflict of interest.

Ethical approval Not applicable.

Consent to participate Not applicable.

Consent for publication Not applicable.

References

- ASTM D1106-21 (2017) Standard test method for acid-insoluble lignin in wood. ASTM International, West Conshohocken
- ASTM D1895-17 (2017) Standard test methods for apparent density, bulk factor, and pourability of plastic materials. ASTM International, West Conshohocken
- ASTM D3173/D3173M-17a (2017) Standard test method for moisture in the analysis sample of coal and coke. ASTM International, West Conshohocken
- ASTM D3174-12 (2018) Standard test method for ash in the analysis sample of coal and coke from coal. ASTM International, West Conshohocken
- ASTM D3175-18 (2018) Standard test method for volatile matter in the analysis sample of coal and coke. ASTM International, West Conshohocken
- Alaylar B, Güllüce M, Egamberdieva D et al (2021) Biochar mediated control of soil-borne phytopathogens. *Environ Sustain* 42(4):329–334. <https://doi.org/10.1007/S42398-021-00187-5>
- Ameloot N, Graber ER, Verheijen FGA, De Neve S (2013) Interactions between biochar stability and soil organisms: review and research needs. *Eur J Soil Sci* 64:379–390. <https://doi.org/10.1111/ejss.12064>
- Antal MJ, Grønli M (2003) The art, science, and technology of charcoal production. *Ind Eng Chem Res* 42:1619–1640
- Beare MH, Gregorich EG, St-Georges P (2009) Compaction effects on CO₂ and N₂O production during drying and rewetting of soil. *Soil Biol Biochem* 41:611–621. <https://doi.org/10.1016/j.soilbio.2008.12.024>
- Binh QA, Nguyen HH (2020) Investigation the isotherm and kinetics of adsorption mechanism of herbicide 2,4-dichlorophenoxyacetic acid (2,4-D) on corn cob biochar. *Bioresour Technol Reports* 11:100520. <https://doi.org/10.1016/J.BITEB.2020.100520>
- Bouaïk H, Tabal A, Barakat A et al (2021) Optimal parameters and structural composition of bio-oil and biochar from intermediate pyrolysis of red algal biomass. *Comptes Rendus Chim* 24:1–15. <https://doi.org/10.5802/CRCHIM.90/>
- Brassard P, Godbout S, Raghavan V et al (2017) The production of engineered biochars in a vertical auger pyrolysis reactor for

- carbon sequestration. *Energies* 10:288. <https://doi.org/10.3390/en10030288>
- Bray R, Kurtz L (1945) Determination of total, organic, and available forms of phosphorus in soils. *Soil Sci* 59:39–46
- Brennan A, Moreno Jiménez E, Alburquerque JA et al (2014) Effects of biochar and activated carbon amendment on maize growth and the uptake and measured availability of polycyclic aromatic hydrocarbons (PAHs) and potentially toxic elements (PTEs). *Environ Pollut* 193:79–87. <https://doi.org/10.1016/j.envpol.2014.06.016>
- Buss W, Mašek O, Graham M, Wüst D (2015) Inherent organic compounds in biochar—their content, composition and potential toxic effects. *J Environ Manag* 156:150–157. <https://doi.org/10.1016/j.jenvman.2015.03.035>
- Chen T, Wu J, Zhang J et al (2014) Gasification kinetic analysis of the three pseudocomponents of biomass—cellulose, hemicellulose and lignin. *Bioresour Technol* 153:223–229. <https://doi.org/10.1016/j.BIORTECH.2013.12.021>
- Chirone R, Salatino P, Scala F (2000) The relevance of attrition to the fate of ashes during fluidized-bed combustion of a biomass. *Proc Combust Inst* 28:2279–2286. [https://doi.org/10.1016/S0082-0784\(00\)80638-4](https://doi.org/10.1016/S0082-0784(00)80638-4)
- Cui S, Ma X, Wang X et al (2019) Phenolic acids derived from rice straw generate peroxides which reduce the viability of *Staphylococcus aureus* cells in biofilm. *Ind Crops Prod* 140:111561. <https://doi.org/10.1016/J.INDCROP.2019.111561>
- Culmo RF, Swanson KJ, Brennan WP (2013) Calculation of weight percentages for organic elemental analysis. *Perkin-Elmer Publ EAN-6*
- Dai Z, Barberán A, Li Y et al (2017) Bacterial community composition associated with pyrogenic organic matter (biochar) varies with pyrolysis temperature and colonization environment. *mSphere*. <https://doi.org/10.1128/msphere.00085-17>
- Egamberdieva D, Zoghi Z, Nazarov K et al (2020) (2020) Plant growth response of broad bean (*Vicia faba* L.) to biochar amendment of loamy sand soil under irrigated and drought conditions. *Environ Sustain* 33(3):319–324. <https://doi.org/10.1007/S42398-020-00116-Y>
- El-Naggar A, Awad YM, Tang X-Y et al (2018) Biochar influences soil carbon pools and facilitates interactions with soil: a field investigation. *Land Degrad Dev* 29:2162–2171. <https://doi.org/10.1002/ldr.2896>
- Gaskin JW, Steiner C, Harris K et al (2008) Effect of low-temperature pyrolysis conditions on biochar for agricultural use. *Trans ASABE* 51:2061–2069. <https://doi.org/10.13031/2013.25409>
- Haque ANA, Uddin MK, Sulaiman MF et al (2021) Biochar with alternate wetting and drying irrigation: a potential technique for paddy soil management. *Agriculture* 367(11):367. <https://doi.org/10.3390/AGRICULTURE11040367>
- Horáček J, Strosser E, Čechová V (2014) arbon fraction concentrations in a haplic Luvisol as affected by tillage. *Plant Soil Environ* 60:262–266. <https://doi.org/10.17221/7416-PSE>
- Huff MD, Marshall S, Saeed HA, Lee JW (2018) Surface oxygenation of biochar through ozonization for dramatically enhancing cation exchange capacity. *Bioresour Bioprocess* 5:18. <https://doi.org/10.1186/s40643-018-0205-9>
- Jackson M (1958) *Soil chemical analysis*. Prentice Hall. Inc., Englewood Cliffs
- Keiluweit M, Nico PS, Johnson M, Kleber M (2010) Dynamic molecular structure of plant biomass-derived black carbon (biochar). *Environ Sci Technol* 44:1247–1253. https://doi.org/10.1021/ES9031419/SUPPL_FILE/ES9031419_SI_001.PDF
- Kolb SE, Fermanich KJ, Dornbush ME (2009) Effect of charcoal quantity on microbial biomass and activity in temperate soils. *Soil Sci Soc Am J* 73:1173–1181. <https://doi.org/10.2136/sssaj2008.0232>
- Kong SH, Loh SK, Bachmann RT et al (2019) Palm kernel shell biochar production, characteristics and carbon sequestration potential. *J Oil Palm Res* 31:508–520. <https://doi.org/10.21894/JOPR.2019.0041>
- Kumar K, Swain AA, Kumar M, Baudh K (2021) Utilization of Eichhornia crassipes biomass for production of biochar and its feasibility in agroecosystems: a review. *Environ Sustain* 42(4):285–297. <https://doi.org/10.1007/S42398-021-00185-7>
- Kuzyakov Y, Subbotina I, Chen H et al (2009) Black carbon decomposition and incorporation into soil microbial biomass estimated by ¹⁴C labeling. *Soil Biol Biochem* 41:210–219. <https://doi.org/10.1016/j.soilbio.2008.10.016>
- Lefèvre R, Barré P, Moyano FE et al (2014) Higher temperature sensitivity for stable than for labile soil organic carbon - Evidence from incubations of long-term bare fallow soils. *Glob Chang Biol* 20:633–640. <https://doi.org/10.1111/gcb.12402>
- Lehmann J, Rillig MC, Thies J et al (2011) Biochar effects on soil biota: a review. *Soil Biol Biochem* 43:1812–1836
- Liang B, Lehmann J, Solomon D et al (2008) Stability of biomass-derived black carbon in soils. *Geochim Cosmochim Acta* 72:6069–6078. <https://doi.org/10.1016/j.gca.2008.09.028>
- Liu X, He Q, Han L et al (2018) The effects of different biochars on microbial quantity, microbial community shift, enzyme activity, and biodegradation of polycyclic aromatic hydrocarbons in soil Mechanochemical degradation of typical persistent organic pollutants enhanced by sulfate radical View project The effects of different biochars on microbial quantity, microbial community shift, enzyme activity, and biodegradation of polycyclic aromatic hydrocarbons in soil. *Artic Geoderma*. <https://doi.org/10.1016/j.geoderma.2018.05.009>
- Luo Y, Durenkamp M, De Nobili M et al (2011) Short term soil priming effects and the mineralisation of biochar following its incorporation to soils of different pH. *Soil Biol Biochem* 43:2304–2314. <https://doi.org/10.1016/j.soilbio.2011.07.020>
- Ma H, Egamberdieva D, Wirth S, Bellingrath-Kimura SD (2019) Effect of biochar and irrigation on soybean-rhizobium symbiotic performance and soil enzymatic activity in field rhizosphere. *Agron* 9:626. <https://doi.org/10.3390/AGRONOMY9100626>
- Maestrini B, Abiven S, Singh N et al (2014) Carbon losses from pyrolysed and original wood in a forest soil under natural and increased N deposition. *Biogeosciences* 11:5199–5213. <https://doi.org/10.5194/bg-11-5199-2014>
- Mukherjee A, Lal R, Zimmerman AR (2014) Impacts of 1.5-year field aging on biochar, humic acid, and water treatment residual amended soil. *Soil Sci* 179:333–339. <https://doi.org/10.1097/SS.0000000000000076>
- Oram NJ, Van de Voorde TFF, Ouwehand GJ et al (2014) Soil amendment with biochar increases the competitive ability of legumes via increased potassium availability. *Agric Ecosyst Environ* 191:92–98. <https://doi.org/10.1016/j.agee.2014.03.031>
- Page A, Miller R, Keeney D (1982) *Methods of soil analysis. Part 2. Chemical and microbiological properties*. Soil Science Society of America, Madison, p 1159
- Pei J, Zhuang S, Cui J, Li J, Li B, Wu J, Fang C (2017) Biochar decreased the temperature sensitivity of soil carbon decomposition in a paddy field. *Agric Ecosyst Environ* 249:156–164
- Puissant J, Jones B, Goodall T et al (2019) The pH optimum of soil exoenzymes adapt to long term changes in soil pH. *Soil Biol Biochem* 138:107601. <https://doi.org/10.1016/j.soilbio.2019.107601>
- Reed ES, Chadwick D, Hill P, Jones D (2016) Soil quality, crop productivity and soil organic matter (SOM) priming in biochar and wood ash amended soils. *Geophys Res Abstr* 18:2016–2523
- Sagrilo E, Jeffery S, Hoffland E, Kuypers TW (2015) Emission of CO₂ from biochar-amended soils and implications for soil organic carbon. *GCB Bioenergy* 7:1294–1304. <https://doi.org/10.1111/gcbb.12234>
- Sarfraz Q, Silva L, Drescher G et al (2020) (2020) Characterization and carbon mineralization of biochars produced from different

- animal manures and plant residues. *Sci Rep* 101(10):1–9. <https://doi.org/10.1038/s41598-020-57987-8>
- Singh B, Singh BP, Cowie AL (2010) Characterisation and evaluation of biochars for their application as a soil amendment. *Soil Res* 48:516. <https://doi.org/10.1071/SR10058>
- Singh BP, Cowie AL, Smernik RJ (2012) Biochar carbon stability in a clayey soil as a function of feedstock and pyrolysis temperature. *Environ Sci Technol* 46:11770–11778. <https://doi.org/10.1021/es302545b>
- Smith JL, Collins HP, Bailey VL (2010) The effect of young biochar on soil respiration. *Soil Biol Biochem* 42:2345–2347. <https://doi.org/10.1016/j.soilbio.2010.09.013>
- Spokas KA (2010) Review of the stability of biochar in soils: Predictability of O: C molar ratios. *Carbon Manag* 1:289–303
- Subbiah B, Asija G (1956) A rapid method for the estimation of nitrogen in soil. *Curr Sci* 26:259–260
- Takaya CA, Fletcher LA, Singh S et al (2016) Phosphate and ammonium sorption capacity of biochar and hydrochar from different wastes. *Chemosphere* 145:518–527. <https://doi.org/10.1016/J.CHEMOSPHERE.2015.11.052>
- Tsai CC, Chang YF (2020) Kinetics of C mineralization of biochars in three excessive compost-fertilized soils: effects of feedstocks and soil properties. *Agron* 10:1749. <https://doi.org/10.3390/AGRON10111749>
- Vance ED, Brookes PC, Jenkinson DS (1987) An extraction method for measuring soil microbial biomass C. *Soil Biol Biochem* 19:703–707. [https://doi.org/10.1016/0038-0717\(87\)90052-6](https://doi.org/10.1016/0038-0717(87)90052-6)
- Ventura M, Zhang C, Baldi E et al (2014) Effect of biochar addition on soil respiration partitioning and root dynamics in an apple orchard. *Eur J Soil Sci* 65:186–195. <https://doi.org/10.1111/ejss.12095>
- Ventura M, Alberti G, Viger M et al (2015) Biochar mineralization and priming effect on SOM decomposition in two European short rotation coppices. *GCB Bioenergy* 7:1150–1160. <https://doi.org/10.1111/GCBB.12219>
- Wang L, Xue C, Nie X et al (2018) Effects of biochar application on soil potassium dynamics and crop uptake. *J Plant Nutr Soil Sci* 181:635–643. <https://doi.org/10.1002/JPLN.201700528>
- Warnock DD, Mummey DL, McBride B et al (2010) Influences of non-herbaceous biochar on arbuscular mycorrhizal fungal abundances in roots and soils: Results from growth-chamber and field experiments. *Appl Soil Ecol* 46:450–456. <https://doi.org/10.1016/j.apsoil.2010.09.002>
- Xiao L, Bi E, Du B et al (2014) Surface characterization of maize-straw-derived biochars and their sorption performance for MTBE and benzene. *Environ Earth Sci* 71:5195–5205. <https://doi.org/10.1007/S12665-013-2922-X/FIGURES/5>
- Yousaf B, Liu G, Wang R et al (2017) Investigating the biochar effects on C-mineralization and sequestration of carbon in soil compared with conventional amendments using the stable isotope ($\delta^{13}C$) approach. *GCB Bioenergy* 9:1085–1099. <https://doi.org/10.1111/GCBB.12401>
- Zhang G, Guo X, Zhu Y et al (2018) The effects of different biochars on microbial quantity, microbial community shift, enzyme activity, and biodegradation of polycyclic aromatic hydrocarbons in soil. *Geoderma* 328:100–108. <https://doi.org/10.1016/j.geoderma.2018.05.009>

Publisher's Note Springer Nature remains neutral with regard to jurisdictional claims in published maps and institutional affiliations.